



Published in final edited form as:

*Epilepsia*. 2020 May ; 61(5): 856–867. doi:10.1111/epi.16490.

## Ictal onset sites and GABAergic neuron loss in epileptic pilocarpine-treated rats

Megan Wyeth<sup>1</sup>, Monica Nagendran<sup>2</sup>, Paul S. Buckmaster<sup>1,3</sup>

<sup>1</sup>Department of Comparative Medicine, Stanford University

<sup>2</sup>Department of Medicine - Pulmonary and Critical Care, Stanford University

<sup>3</sup>Department of Neurology & Neurological Sciences, Stanford University, Stanford University

### Summary

**Objective**—The present study tested whether ictal onset sites are regions of more severe interneuron loss in epileptic pilocarpine-treated rats, a model of human temporal lobe epilepsy.

**Methods**—Local field potential recordings were evaluated to identify ictal onset sites. Electrode sites were visualized in Nissl-stained sections. Adjacent sections were processed with proximity ligation *in situ* hybridization for glutamic acid decarboxylase 2 (*Gad2*). *Gad2* neuron profile numbers at ictal onset sites were compared to contralateral regions. Other sections were processed with immunocytochemistry for reelin or nitric oxide synthase (NOS) which labeled major subtypes of granule cell layer-associated interneurons. Stereology was used to estimate numbers of reelin and NOS granule cell layer-associated interneurons per hippocampus.

**Results**—Ictal onset sites varied between and within rats but were mostly in the ventral hippocampus and were frequently bilateral. There was no conclusive evidence of more severe *Gad2* neuron profile loss at sites of earliest seizure activity compared to contralateral regions. Numbers of granule cell layer-associated NOS neurons were reduced in the ventral hippocampus.

**Significance**—In epileptic pilocarpine-treated rats, ictal onset sites were mostly in the ventral hippocampus where there was loss of granule cell layer-associated NOS interneurons. These findings suggest the hypothesis that loss of granule cell layer-associated NOS interneurons in the ventral hippocampus is a mechanism of temporal lobe epilepsy.

### Keywords

seizure; focus; interneuron; epilepsy; hippocampus

---

Corresponding author: Paul Buckmaster, 300 Pasteur Drive, Department of Comparative Medicine, R321 Edwards Building, Stanford University, Stanford, CA 94305, (650)498-4774, (650)498-5085(fax), psb@stanford.edu.

#### Disclosure

None of the authors has any conflict of interest to disclose.

#### Ethical Publication Statement

We confirm that we have read the Journal's position on issues involved in ethical publication and affirm that this report is consistent with those guidelines.

## Introduction

Many questions persist about mechanisms of temporal lobe epilepsy. How do spontaneous seizures initiate? Do seizures start at a consistent focus, across a more distributed network, or both? An experimental model that might help answer these questions are rats that develop epilepsy after systemic treatment with pilocarpine to cause status epilepticus<sup>1</sup>. In epileptic pilocarpine-treated rats and in human patients with temporal lobe epilepsy the most epileptogenic zone is a homologous region: ventral hippocampus in rats<sup>2</sup>, anterior hippocampus in humans<sup>3-5</sup>. Hippocampal sclerosis is bilateral in 25% of human patients<sup>6</sup>. In epileptic pilocarpine-treated rats, the degree to which seizures start unilaterally, bilaterally, or both is unclear. Addressing that would help investigators target ictal onset sites in their experiments.

GABAergic neuron loss occurs in the dentate gyrus of patients with temporal lobe epilepsy<sup>7-12</sup> and in animal models<sup>13-21</sup>. Functionally, dentate granule cells display reduced inhibitory synaptic input in patients with temporal lobe epilepsy<sup>22</sup> and in epileptic rats<sup>20,23,24</sup>. In epileptic pilocarpine-treated mice, seizure frequency correlates with loss of granule cell layer-associated GABAergic neurons<sup>25</sup>, and transplanting GABAergic neuron progenitors into the hippocampus reduces seizure frequency<sup>26</sup>. The present study tested whether ictal onset sites in epileptic pilocarpine-treated rats are regions of more severe interneuron loss.

## Methods

### Animals

**Pilocarpine treatment**—All experiments were performed in accordance with the National Institutes of Health Guide for the Care and Use of Laboratory Animals and were approved by a Stanford University Institutional Animal Care and Use Committee. When they were 34–41 d old, male and female Sprague-Dawley rats were treated with pilocarpine hydrochloride (380 mg/kg, intraperitoneal) administered 20 min after atropine methyl bromide (5 mg/kg, intraperitoneal). Sixty two percent of the rats treated with pilocarpine developed status epilepticus. Diazepam (10 mg/kg, intraperitoneal) was administered 2 h after the onset of motor seizures and was repeated as needed for the next 10 h to suppress convulsions. Ten percent of the rats that developed status epilepticus died. Eleven percent of the rats that did not develop status epilepticus did display one convulsive seizure the day of pilocarpine treatment. However, none of the rats that failed to develop status epilepticus was observed to experience seizures in the following months. To reduce the number of animals used, the implanted control group consisted of rats that had been treated identically with pilocarpine but did not develop status epilepticus.

**Surgery**—Rats were implanted with electrodes  $9 \pm 1$  months (mean  $\pm$  s.e.m.) after pilocarpine-treatment. Rats were sedated with diazepam (5 mg/kg, intraperitoneal), anesthetized with isoflurane (1.5%), placed in a stereotaxic frame, maintained on a heating pad with feedback control, given antibiotic (enrofloxacin, 10 mg/kg, subcutaneous), lactated Ringer's solution (10 ml, subcutaneous) and analgesic (carprofen, 5 mg/kg, subcutaneous), and prepared for aseptic surgery. Bipolar electrodes consisted of 25  $\mu$ m diameter H-formvar-

coated stainless steel wires (California Wire Company) glued together with tips 1 mm apart. Electrodes were directed toward the following regions bilaterally (anterior-posterior and medial-lateral stereotactic coordinates in mm referenced to bregma and to the brain surface): septum (medial and lateral parts and the diagonal band of Broca) (0.7, 0.3, 5.9), amygdala (including the cortex-amygdala transition zone and amygdaloid-hippocampus) (-2.8, 4.4, 7.9), olfactory cortex (including the endopiriform nucleus, postpiriform transition area, and olfactory tubercle) (-2.8, 5.8, 7.4), dorsal hippocampus (dentate gyrus and CA1-3) (-4.6, 2.6, 3.1), ventral hippocampus (-5.5, 4.8, 7.1), ventral subiculum (-6.6, 4.6, 7.5), and entorhinal cortex (medial and lateral parts) (-7.9, 5.0, 5.3). A reference electrode was placed in the cerebellum. The ground consisted of screws in the skull caudal to lambda. Electrodes were connected to an interface board (EIB-36-9 drive, Neuralynx) on an aluminum ring affixed to the skull with cranioplastic cement and jeweler's screws.

### Recording and analysis

Local field potential and time-locked video recording began at least 7 d after surgery. Recordings were obtained as rats rested in a cage during the day ( $9.8 \pm 0.1$  h/d) for  $16.1 \pm 3.4$  (range, 5–43) days. Signals were buffered with a headstage (HS-36, Neuralynx), amplified, digitized, filtered (0.1–1,800 Hz), sampled (2000 Hz) (Cheetah Data Acquisition, Neuralynx), and saved for off-line analysis.

Seizures were included for analysis if they were at least 10 s in duration. For each seizure, the channel that displayed the earliest persistent change that developed into clear seizure activity was identified by a single investigator (P.S.B.) who was blind to electrode locations. At the 2000 Hz sampling rate, it was almost always possible to identify a single channel with the earliest seizure onset. On rare occasions, when two channels had simultaneous onsets, the channel with the largest amplitude deflection relative to its pre-seizure baseline activity was selected as the onset channel. This manual method was used because it was previously found to be more reliable than automated approaches<sup>2</sup>. More complicated analyses that identify epileptogenic zones by evaluating features that extend beyond the earliest evidence of seizure onset are under development and might be useful in future studies<sup>27</sup>.

### Anatomy

After recordings were completed, rats were killed with pentobarbital (>100 mg/kg, intraperitoneal) and perfused at 30 ml/min through the ascending aorta for 1 min with 0.9% NaCl and 30 min with 4% formaldehyde in 0.1 M phosphate buffer (PB, pH 7.4). Brains were removed and stored in fixative at 4°C at least overnight, equilibrated in 30% sucrose in PB, and sectioned coronally using a sliding microtome set at 40  $\mu$ m. Every other section was Nissl-stained with 0.25% thionin to visualize electrode tracks.

**In situ hybridization**—GABAergic neurons were labeled for expression of glutamic acid decarboxylase 2 (*Gad2*) mRNA using proximity ligation *in situ* hybridization<sup>28</sup>. Free-floating sections were rinsed in phosphate buffered saline (PBS) then pretreated with 0.2 N HCl for 10 min, followed by 3 min in 0.01% Triton-X 100 at room temperature. After rinsing, pretreatment continued with 0.25  $\mu$ g/ml Proteinase K with 5 mM EDTA in 50 mM

Tris (pH 7.4) for 10 min, then two 3 min incubations in 2 mg/ml glycine, both at 37°C. Two adjacent 20 base pair probes targeted 40 base pair sections of rat *Gad2*. See Supporting Information for probe sequences. For hybridization, sections were incubated in a solution containing 5 probe pairs (100 nM each) in hybridization buffer (1 M sodium trichloroacetate, 5 mM EDTA, and 0.2 mg/ml heparin in Tris) with 100 mM dithiothreitol and 10 mg/ml tRNA for 2 h at 37°C. Sections were rinsed in hybridization buffer at 37°C before incubation in a solution containing phosphorylated “bridge” oligos (120 nM) that bind the *Gad2* probe pairs and “circle” oligos (120 nM) with a target sequence for the label probe suspended in Ligase Buffer with 10 mM ATP (New England Biolabs) in addition to 0.4 mg/ml bovine serum albumin (BSA), 0.2 mg/ml heparin, 0.25 M NaCl, and 0.005% Tween-20 for 1 h at 37°C. Sections were briefly rinsed in PBS with 0.5% Tween-20 before the ligation reaction to join the bridge and circle oligos. For this, sections were incubated in a solution containing 10,000 units/ml T4 DNA Ligase in Ligase Buffer with 10 mM ATP (New England Biolabs) together with 0.4 units/μl RNaseOUT (Invitrogen), 0.4 mg/ml BSA, 0.25 NaCl, and 0.005% Tween-20 for 2 h at 37°C. Sections were rinsed in hybridization buffer followed by phi29 polymerase buffer before the rolling circle amplification reaction. Amplification solution contained 1000 units/ml NxGen phi29 DNA polymerase in phi29 polymerase buffer (Lucigen) and 1 mM dNTP mix (0.25 mM/nucleotide, Invitrogen), 0.4 units/μl RNaseOUT, 5% glycerol, and 0.4 mg/ml BSA; sections incubated overnight at 37°C. The next day sections were rinsed in a label probe hybridization buffer of 2x saline-sodium citrate (Invitrogen) and 20% deionized formamide (Invitrogen) in DEPC-treated water. Sections were finally incubated with the detection oligo conjugated to Cy5 (100 nM) in the label probe hybridization buffer along with 0.2 mg/ml heparin for 1 h at 37°C, before rinsing with PBS, labeling with DAPI, mounting, and coverslipping. Sections were imaged with a Nikon A-1 confocal microscope.

**Immunocytochemistry**—In unimplanted control rats, hippocampi were isolated and sectioned transversely along the septotemporal axis. Adjacent 1-in-24 series of sections were processed for reelin (RLN, Abcam, ab78540, 1:8000), somatostatin (Peninsula, T-4103, 1:32,000), parvalbumin (Swant, PV27, 1:80,000), nitric oxide synthase (NOS, Sigma, N7280, 1:64,000), cholecystinin (Center for Ulcer Research and Education, UCLA, 9303, 1:10,000), calretinin (Swant, CR7697, 1:32,000), or vasoactive intestinal polypeptide (Immunostar, 20077, 1:4000) using an established protocol and optical fractionator method to estimate the number of interneurons per hippocampus<sup>25</sup>. Neuron somata were counted if they were in or adjacent to the granule cell layer and were not cut at the surface of the section.

From each of the electrode-implanted control and epileptic rats, 1-in-8 series of coronal sections were processed for RLN- or NOS-immunoreactivity. Immunoreactive neuron profiles in or adjacent to the granule cell layer were counted. A method was devised to convert data from coronal sections to plots along the septotemporal axis of the hippocampus (Figure 5E). In coronal sections, the septal hippocampus is dorsal: the temporal hippocampus is ventral. Caudally the dorsal and ventral parts become contiguous. Here, dorsal and ventral halves were defined by drawing a perpendicular line equidistant from a line connecting the dorsal tip of the granule cell layer to the ventral tip. To estimate numbers

of neurons per hippocampus from profile counts, five hippocampi with a broad range of profile counts were evaluated using the optical fractionator method to generate a plot of profiles versus neurons per dentate gyrus. Regression line ( $r > 0.93$ ) slopes were used to convert profile counts to neurons per hippocampus for all samples.

## Statistics

Sigma Plot 12 was used for statistical analyses, and  $p < 0.05$  was considered significant. To test if the observed number of earliest recorded seizure onsets exceeded that expected by chance, based on the number of recording electrodes in a region, z-scores were calculated according to the following formula:

$$z = \frac{p' - p}{\sqrt{\frac{pq}{n}}}$$

where  $p'$  = observed probability of earliest seizure onset,  $p$  = expected probability of earliest seizure onset if random (= number of electrodes in that brain region / total number of electrodes),  $q = p-1$ ,  $n$  = number of seizures. Z-scores  $> 1.96$  were significant ( $p < 0.05$ )<sup>29</sup>.

## Results

### Ictal onset sites

In each rat, 28 electrodes (14 bipolar) were implanted, and there were  $23.5 \pm 4.2$  useful electrodes/rat,  $20.2 \pm 3.7$  in targeted regions (Table 1). A total of 1451 seizures were analyzed,  $112 \pm 19$  per rat. No region displayed the earliest seizure activity with 100% consistency in any of the rats. For example, of the 109 seizures recorded in rat #1, 48% were earliest in the left ventral subiculum, 43% in the right ventral subiculum, and 9% in the left dorsal hippocampus (Figure 1). Between 13 rats with seven regions targeted bilaterally, 143 targeted regions were recorded and 65% displayed the earliest seizure activity at least once. Of 16 electrodes in the septum for the group, five recorded the earliest seizure activity at least once. The septum had the lowest proportion of earliest seizure recordings per number of recording sites (5/16); the ventral hippocampus had the highest (19/20).

In all epileptic rats, a subset of regions had significantly more onsets than expected by chance. In rat #2 for example, 7/13 targeted regions had at least one earliest recorded seizure (Table 1). Of those, more onsets than expected by chance occurred in three: the left ventral hippocampus (8% of onsets), left subiculum (16%), and right ventral hippocampus (66%) which had the maximum z-score in this animal (Figure 2). The right ventral hippocampus contained four electrodes, one of which recorded almost all of the onsets. For the group, there were  $2.5 \pm 0.3$  sites/rat that were more likely than chance to display earliest seizure activity. Individual significantly early sites accounted for  $30 \pm 3\%$  (range 8–70%) of seizures/rat. Summing all significantly early sites/rat accounted for  $75 \pm 4\%$  (range 47–96%) of seizures. The septum was the site with the lowest proportion of significant onsets recorded (0/16), and the ventral hippocampus had the highest (15/20). The ventral hippocampus also had the maximum z-score in 6/13 rats, and in three more rats the ventral subiculum had the maximum z-score.

There were significantly early sites on both sides of the brain in 11/13 rats (Table 1). In 7 rats these sites included those in the same brain region, and in 5 rats this included the region contralateral to the region with the maximum z-score. For the group, there were 22 cases in which there was a significantly early site and bilateral electrodes for that region. Significantly early sites were unilateral in the olfactory cortex (1 case), entorhinal cortex (1), and dorsal hippocampus (4). Bilateral significantly early sites occurred in a subset of cases in the amygdala (1/3), ventral subiculum (1/5), and especially in the ventral hippocampus (5/8).

### Gad2 neurons

In some cases, a single electrode could record almost all of the earliest seizure activity within a brain region that contained multiple electrodes (Figure 2), suggesting specificity to that electrode location. Brain regions with at least two electrodes and at least ten significantly earliest seizure recordings were further evaluated for subregion specificity. Of 79 electrodes in those regions, 15 recorded at least twice as many seizures earlier than expected by chance for the number of electrodes in that region, and seven recorded all in their region. This raises the possibility that an ictal onset zone can be as small as the space between closest electrodes (1 mm) or that it can be defined by sharp borders. To test ictal onset sites for more severe loss of GABAergic neurons, electrodes with the highest z-scores for earliest seizure activity were identified (Table 1). For those electrodes, the section including the recording site or within four sections (160  $\mu\text{m}$ ) was evaluated by counting the number of *Gad2*-positive neuron profiles within a radius of 250  $\mu\text{m}$  from the electrode tip (Figure 3), since local field potential electrodes are estimated to record signals within 250  $\mu\text{m}$ <sup>30,31</sup>.

The new PLISH method<sup>28</sup> was validated by confirming the expected *Gad2* expression pattern in the dentate gyrus of control rats (Figure 3B). The number of *Gad2* profiles/ $\text{mm}^2$  was similar at highest z-score sites ( $67.4 \pm 17.0$ ) and contralaterally ( $65.4 \pm 19.4$ ,  $p = 0.83$ , paired t test). Interneuron axons project beyond 250  $\mu\text{m}$ , so a broader region was evaluated ( $1.6 \times 1.6$  mm). Again, the number of profiles/ $\text{mm}^2$  at highest z-score sites ( $53.4 \pm 8.2$ ) was not significantly less than contralaterally ( $64.4 \pm 17.5$ ,  $p = 0.34$ , Wilcoxon signed rank test). In some cases, the contralateral region also was a site of significantly earliest recorded seizure activity. Eliminating those cases did not change the conclusion: numbers of profiles/ $\text{mm}^2$  at highest z-score sites versus contralateral sites were similar within a 250  $\mu\text{m}$  radius ( $93.4 \pm 28.8$  versus  $93.4 \pm 38.7$ ,  $p = 0.50$ , paired t test). In the broader  $1.6 \times 1.6$  mm region *Gad2* neuron profile density was lower at highest z-score sites ( $66.2 \pm 13.1$ ) compared to contralateral sites ( $90.7 \pm 35.6$ ), but the difference was not significant ( $p = 0.31$ , Wilcoxon signed rank test), and statistical power was limited.

### Granule cell layer-associated interneurons

The ventral hippocampus was the most frequent site of earliest seizure activity, and seizure frequency correlates with loss of granule cell layer-associated GABAergic neurons<sup>25</sup>, so granule cell layer-associated interneurons were evaluated. Seven major subtypes were quantified in unimplanted control rats ( $n = 3$ ) (Figure 4). There were  $14,600 \pm 700$  RLN- and  $8120 \pm 100$  NOS-positive granule cell layer-associated interneurons per hippocampus.



All other tested interneuron types were less than 3000 and therefore unlikely to account for the quantitative loss that correlates with seizure frequency.

RLN and NOS interneurons were evaluated in implanted control ( $n = 12$ ) and epileptic rats. The number of granule cell layer-associated interneuron profiles per section was plotted separating dorsal and ventral parts of the hippocampus along the x-axis (Figure 5). The number of granule cell layer-associated RLN interneurons per dentate gyrus in control rats was  $14,700 \pm 400$ . In epileptic rats, their number was reduced to 86% of controls ( $12,600 \pm 600$ ,  $p < 0.001$ , t test). The reduction was attributable to fewer cells in the dorsal hippocampus ( $7220 \pm 330$  versus  $9130 \pm 300$ ,  $p < 0.001$ ). The plot of RLN profiles/section in the ventral hippocampus of epileptic rats was shorter but broader than controls, suggesting changes in the shape of the hippocampus. There was no significant reduction per ventral hippocampus ( $5380 \pm 280$  versus  $5560 \pm 220$ ,  $p = 0.62$ ).

The number of granule cell layer-associated NOS interneurons per dentate gyrus in control rats was  $8550 \pm 330$ . In epileptic rats, their number was reduced to 65% of controls ( $5580 \pm 460$ ,  $p < 0.001$ ). The reduction was attributable to fewer cells in both the dorsal ( $3840 \pm 300$  versus  $5570 \pm 210$ ,  $p < 0.001$ ) and ventral hippocampus ( $1730 \pm 180$  versus  $2990 \pm 170$ ,  $p < 0.001$ ) where the average was reduced to 58% of controls. Ventral hippocampi that were sites of significantly earliest recorded seizure activity had fewer granule cell layer-associated NOS neurons ( $1450 \pm 120$ ) than ventral hippocampi that were not ( $1840 \pm 380$ ), but the difference was not significant ( $p = 0.32$ ), and sample size and statistical power were limited.

## Discussion

The principal findings were that in epileptic pilocarpine-treated rats ictal onset sites were mostly in the ventral hippocampus and frequently bilateral. The parameter of interneuron loss that colocalized best with ictal onset sites was loss of granule cell layer-associated NOS neurons.

### Ictal onset sites

Challenges of identifying ictal onset sites have been described<sup>32</sup>. One is sparse spatial sampling, raising the possibility that a seizure actually began in an unrecorded area. As described previously, the local field potential recording scheme employed in the present study might sample only 0.1% of a rat's brain<sup>2</sup>. Another is rapid spread of seizure activity. Compared to human patients with temporal lobe epilepsy, seizures in pilocarpine-treated rats spread faster, and the reason for the difference is unclear<sup>2</sup>. We attempted to address these challenges by recording up to 186 seizures/rat, targeting seven potentially ictogenic regions, recording with submillisecond temporal resolution, analyzing earliest seizure activity while blind to electrode locations, and statistically testing whether the number of earliest seizure recordings was above chance levels. Results confirmed that the ventral hippocampus is a likely ictal onset site and revealed that in the ventral hippocampus, ictal onset sites are frequently bilateral.

All rats displayed multiple ictal onset sites. Similar variability has been reported in human patients<sup>33-35</sup> and in other rat models<sup>36</sup>. This finding is consistent with the view that seizures

are generated by multiple foci or a network of interlinked seizure-initiating sites<sup>37,38</sup>. It remains unclear whether ictogenic network nodes are interdependent or can independently generate seizures. Rats in the present study were evaluated months after pilocarpine treatment. It is possible that there would be fewer seizure foci earlier in the epileptogenic process<sup>36</sup>. In some cases, an electrode only 1 mm away from another accounted for a large proportion of the ictal onsets. This finding is consistent with previous reports that ictal onset sites can be quite small<sup>39–42</sup>.

### Interneuron loss

A challenge of identifying mechanisms of temporal lobe epilepsy is the abundance of abnormalities that have been discovered in tissue from patients and in animal models. The abundance has spawned many hypotheses. One is that interneuron loss reduces inhibition of excitatory neurons, which lowers seizure threshold (see Introduction). The present study tested whether interneuron loss was more severe at ictal onset sites. *Gad2* neuron profile density was not significantly reduced at narrowly defined ictal onset sites (electrode-centered). More specific analysis was performed on RLN- and NOS-positive neurons. Both are GABAergic<sup>43,44</sup> and have been reported to be reduced in the dentate gyrus in rodent models of temporal lobe epilepsy<sup>45–49</sup>. The present study discovered that NOS- but not RLN-positive granule cell layer-associated interneurons were significantly reduced in the ventral hippocampus, the most common ictal onset site (regionally defined). In the ventral hippocampus of rodent models of temporal lobe epilepsy there is loss of other dentate gyrus interneurons including parvalbumin interneurons<sup>15,16,18,20</sup>, but loss of those interneuron subtypes has not been shown to correlate with seizure frequency<sup>25</sup> (and correlation with interneuron loss outside the dentate gyrus has not been tested). Granule cell layer-associated NOS neurons are reduced in patients with temporal lobe epilepsy<sup>50</sup>. More work is needed to further test the role of ventral granule cell layer-associated NOS neuron loss in temporal lobe epileptogenesis.

### Supplementary Material

Refer to Web version on PubMed Central for supplementary material.

### Acknowledgments

Funded by NIH/NINDS.

### References

1. Turski L, Ikonomidou C, Turski WA, et al. Review: cholinergic mechanisms and epileptogenesis. The seizures induced by pilocarpine: a novel experimental model of intractable epilepsy. *Synapse* 1989;3:154–171. [PubMed: 2648633]
2. Toyoda I, Bower MR, Leyva F, et al. Early activation of ventral hippocampus and subiculum during spontaneous seizures in a rat model of temporal lobe epilepsy. *J Neurosci* 2013;33:11100–11115. [PubMed: 23825415]
3. King DW, Ajmone Marsan C. Clinical features and ictal patterns in epileptic patients with EEG temporal lobe foci. *Ann Neurol* 1977;2:138–147.



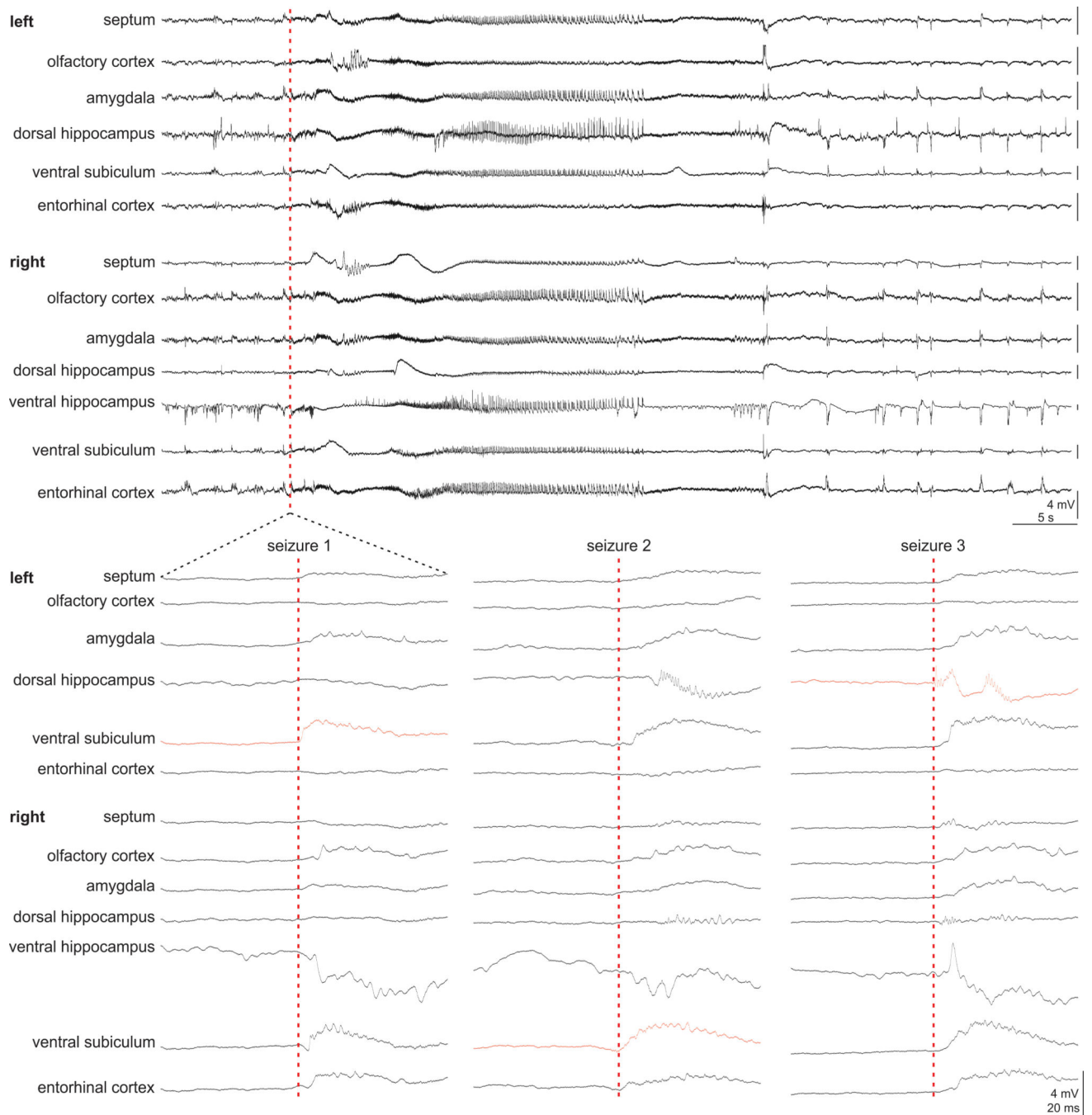
4. Masukawa LM, O'Connor WM, Lynott J, et al. Longitudinal variation in cell density and mossy fiber reorganization in the dentate gyrus from temporal lobe epileptic patients. *Brain Res* 1995;678:65–75. [PubMed: 7620900]
5. King D, Bronen RA, Spencer DD, et al. Topographic distribution of seizure onset and hippocampal atrophy: relationship between MRI and depth EEG. *Electroencephalogr Clin Neurophysiol* 1997;103:692–697. [PubMed: 9546496]
6. Briellmann RS, Jackson GD, Mitchell LA, et al. Occurrence of hippocampal sclerosis: is one hemisphere or gender more vulnerable? *Epilepsia* 1999;40:1816–1820. [PubMed: 10612350]
7. de Lanerolle NC, Kim JH, Robbins RJ, et al. Hippocampal interneuron loss and plasticity in human temporal lobe epilepsy. *Brain Res* 1989;495:387–395. [PubMed: 2569920]
8. Sloviter RS. Permanently altered hippocampal structure, excitability, and inhibition after experimental status epilepticus in the rat: the “dormant basket cell” hypothesis and its possible relevance to temporal lobe epilepsy. *Hippocampus* 1991;1:41–66. [PubMed: 1688284]
9. Mathern GW, Babb TL, Pretorius JK, et al. Reactive synaptogenesis and neuron densities for neuropeptide Y, somatostatin, and glutamate decarboxylase immunoreactivity in the epileptogenic human fascia dentata. *J Neurosci* 1995;15:3990–4004. [PubMed: 7751960]
10. Zhu ZQ, Armstrong DL, Hamilton WJ, et al. Disproportionate loss of CA4 parvalbumin-immunoreactive interneurons in patients with Ammon’s horn sclerosis. *J Neuropathol Exp Neurol* 1997;56:988–998. [PubMed: 9291940]
11. Zs Maglóczy, Wittner L Borhegyi Zs, et al. Changes in the distribution and connectivity of interneurons in the epileptic human dentate gyrus. *Neuroscience* 2000;96:7–25. [PubMed: 10683405]
12. Andrioli A, Alonso-Nanclares L, Arellano JI, et al. Quantitative analysis of parvalbumin-immunoreactive cells in the human epileptic hippocampus. *Neuroscience* 2007;149:131–143. [PubMed: 17850980]
13. Freund TF, Ylinen A, Miettinen R, et al. Pattern of neuronal death in the rat hippocampus after status epilepticus. Relationship to calcium binding protein content and ischemic vulnerability. *Brain Res Bull* 1991;28:27–38.
14. Obenaus A, Esclapez M, Houser CR. Loss of glutamate decarboxylase mRNA-containing neurons in the rat dentate gyrus following pilocarpine-induced seizures. *J Neurosci* 1993;13:4470–4485. [PubMed: 8410199]
15. Schwarzer C, Williamson JM, Lothman EW, et al. Somatostatin, neuropeptide Y, neurokinin B and cholecystokinin immunoreactivity in two chronic models of temporal lobe epilepsy. *Neuroscience* 1995;69:831–845. [PubMed: 8596652]
16. Buckmaster PS, Dudek FE. Neuron loss, granule cell axon reorganization, and functional changes in the dentate gyrus of epileptic kainate-treated rats. *J Comp Neurol* 1997;385:385–404. [PubMed: 9300766]
17. André V, Marescaux C, Nehlig A, et al. Alterations of hippocampal GABAergic system contribute to development of spontaneous recurrent seizures in the rat lithium-pilocarpine model of temporal lobe epilepsy. *Hippocampus* 2001;11:452–468. [PubMed: 11530850]
18. Gorter JA, van Vliet EA, Aronica E, et al. Progression of spontaneous seizures after status epilepticus is associated with mossy fibre sprouting and extensive bilateral loss of hilar parvalbumin and somatostatin-immunoreactive neurons. *Eur J Neurosci* 2001;13:657–669. [PubMed: 11207801]
19. Sayin U, Osting S, Hagen J, et al. Spontaneous seizures and loss of axo-axonic and axo-somatic inhibition induced by repeated brief seizures in kindled rats. *J Neurosci* 2003;23:2759–2768. [PubMed: 12684462]
20. Sun C, Mchedlishvili Z, Bertram EH, et al. Selective loss of dentate hilar interneurons contributes to reduced synaptic inhibition of granule cells in an electrical stimulation-based animal model of temporal lobe epilepsy. *J Comp Neurol* 2007;500:876–893. [PubMed: 17177260]
21. Huusko N, Römer C, Ndode-Ekane XE, et al. Loss of hippocampal interneurons and epileptogenesis: a comparison of two animal models of acquired epilepsy. *Brain Struct Funct* 2015;220:153–191. [PubMed: 24096381]

22. Williamson A, Patrylo PR, Spencer DD. Decrease in inhibition in dentate granule cells from patients with medial temporal lobe epilepsy. *Ann Neurol* 1999;45:92–99. [PubMed: 9894882]
23. Kobayashi M, Buckmaster PS. Reduced inhibition of dentate granule cells in a model of temporal lobe epilepsy. *J Neurosci* 2003;23:2440–2452. [PubMed: 12657704]
24. Shao L-R, Dudek FE. Changes in mIPSCs and sIPSCs after kainate treatment: evidence for loss of inhibitory input to dentate granule cells and possible compensatory responses. *J Neurophysiol* 2005;94:952–960. [PubMed: 15772233]
25. Buckmaster PS, Abrams E, Wen X. Seizure frequency correlates with loss of dentate gyrus GABAergic neurons in a mouse model of temporal lobe epilepsy. *J Comp Neurol* 2017;525:2592–2610. [PubMed: 28425097]
26. Hunt RF, Girskis KM, Rubenstein JL, et al. GABA progenitors grafted into the adult epileptic brain control seizures and abnormal behavior. *Nat Neurosci* 2013;16:692–697. [PubMed: 23644485]
27. Grinenko O, Li J, Mosher JC, et al. A fingerprint of the epileptogenic zone in human epilepsies. *Brain* 2018;141:117–131.
28. Nagendran M, Riordan DP, Harbury PB, et al. Automated cell-type classification in intact tissues by single-cell molecular profiling. *Elife* 2018;e30510. [PubMed: 29319504]
29. Daniel WW. *Biostatistics: a foundation for analysis in the health sciences*. 4th edition New York: Wiley; 1987.
30. Katzner S, Nauhaus I, Benucci A, et al. Local origin of field potentials in visual cortex. *Neuron* 2009;61:35–41. [PubMed: 19146811]
31. Xing D, Yeh CI, Shapley RM. Spatial spread of the local field potential and its laminar variation in visual cortex. *J Neurosci* 2009;29:11540–11549. [PubMed: 19759301]
32. Rosenow F, Lüders H. Presurgical evaluation of epilepsy. *Brain* 2001;124:1683–1700. [PubMed: 11522572]
33. Lieb JP, Walsh GO, Babb TL, et al. A comparison of EEG seizure patterns recorded with surface and depth electrodes in patients with temporal lobe epilepsy. *Epilepsia* 1976;17:137–160. [PubMed: 947745]
34. Spencer SS, Spencer DD, Williamson PD, et al. Combined depth and subdural electrode investigation in uncontrolled epilepsy. *Neurology* 1990;40:74–79. [PubMed: 2296386]
35. Spencer SS, Spencer DD. Entorhinal-hippocampal interactions in medial temporal lobe epilepsy. *Epilepsia* 1994;35:721–727. [PubMed: 8082614]
36. Bertram EH. Functional anatomy of spontaneous seizures in a rat model of limbic epilepsy. *Epilepsia* 1997;38:95–105. [PubMed: 9024190]
37. Spencer SS. Neural networks in human epilepsy: evidence of and implications for treatment. *Epilepsia* 2002;43:219–227. [PubMed: 11906505]
38. Bartolomei F, Lagarde S, Wendling F, et al. Defining epileptogenic networks: contribution of SEEG and signal analysis. *Epilepsia* 2017;58:1131–1147. [PubMed: 28543030]
39. Bragin A, Engel J Jr, Wilson CL, et al. Electrophysiologic analysis of a chronic seizure model after unilateral hippocampal KA injection. *Epilepsia* 1999;40:1210–1221. [PubMed: 10487183]
40. Schevon CA, Ng SK, Cappell J, et al. Microphysiology of epileptiform activity in human neocortex. *J Clin Neurophysiol* 2008;25:321–330. [PubMed: 18997628]
41. Worrell GA, Gardner AB, Stead SM, et al. High-frequency oscillations in human temporal lobe: simultaneous microwire and clinical macroelectrode recordings. *Brain* 2008;131:928–937. [PubMed: 18263625]
42. Stead M, Bower M, Brinkmann BH, et al. Microseizures and the spatiotemporal scales of human partial epilepsy. *Brain* 2010;133:2789–2797. [PubMed: 20685804]
43. Valtchanoff JG, Weinberg RJ, Kharazia VN, et al. Neurons in rat hippocampus that synthesize nitric oxide. *J Comp Neurol* 1993;331:111–121. [PubMed: 7686569]
44. Pesold C, Impagnatiello F, Pisu MG, et al. Reelin is preferentially expressed in neurons synthesizing  $\gamma$ -aminobutyric acid in cortex and hippocampus of adult rats. *Proc Natl Acad Sci USA* 1998;95:3221–3226. [PubMed: 9501244]

45. Kotti T, Halonen T, Sirviö, et al. Comparison of NADPH diaphorase histochemistry, somatostatin immunohistochemistry, and silver impregnation in detecting structural and functional impairment in experimental status epilepticus. *Neuroscience* 1997;30:105–117.
46. Hamani C, Tenório F, Mendez-Otero R, et al. Loss of NADPH diaphorase-positive neurons in the hippocampal formation of chronic pilocarpine-epileptic rats. *Hippocampus* 1999;9:303–313. [PubMed: 10401644]
47. Gong C, Wang TW, Huang HS, et al. Reelin regulates neuronal progenitor migration in intact and epileptic hippocampus. *J Neurosci* 2007;27:1803–1811. [PubMed: 17314278]
48. Fournier NM, Andersen DR, Botterill JJ, et al. The effect of amygdala kindling on hippocampal neurogenesis coincides with decreased reelin and DISC1 expression in the adult dentate gyrus. *Hippocampus* 2010;20:659–671. [PubMed: 19499587]
49. Mishra V, Shuai B, Kodali M, et al. Resveratrol treatment after status epilepticus restrains neurodegeneration and abnormal neurogenesis with suppression of oxidative stress and inflammation. *Scientific Reports* 2015;5:17807. [PubMed: 26639668]
50. Leite JP, Chimelli L, Terra-Bustamante VC, et al. Loss and sprouting of nitric oxide synthase neurons in the human epileptic hippocampus. *Epilepsia* 2002;43(suppl):235–242. [PubMed: 12121328]

**Key Points**

- Pilocarpine-treated rats display multiple ictal onset sites.
- The ventral hippocampus is the most common ictal onset site.
- Ictal onset sites are frequently bilateral in the ventral hippocampus.
- Reelin and NOS-positive neurons are the most abundant granule cell layer-associated interneurons.
- Epileptic rats display substantial loss of granule cell layer-associated NOS interneurons in the ventral hippocampus.

**Figure 1.**

Earliest recorded seizure activity at multiple sites in an epileptic pilocarpine-treated rat. **A** Seizure onset indicated by red dashed line. **B** Seizure 1 is an expanded view that reveals earliest recorded seizure activity in the left ventral subiculum. The high-amplitude background activity in the right ventral hippocampus should not be confused with the seizure onset. Seizures 2 and 3 show onsets of two other seizures recorded on another day. The earliest recorded seizure activity was in the right ventral subiculum of seizure 2 and the left dorsal hippocampus of seizure 3.

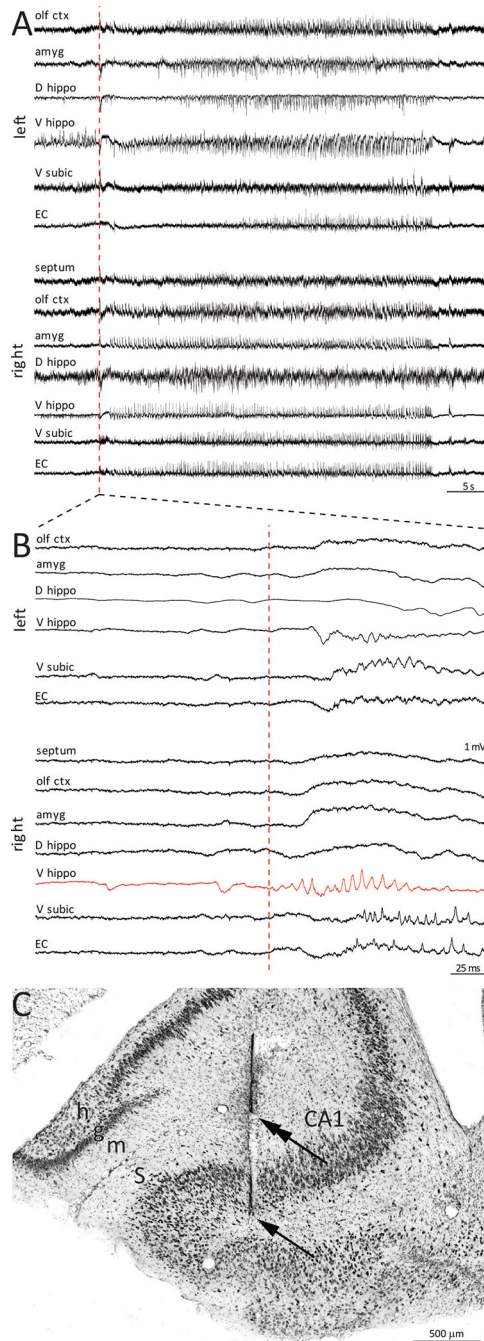


**Figure 2.**

Earliest recorded seizure activity in the ventral hippocampus. **A** Seizure onset indicated by red dashed line. **B** Expanded view reveals earliest seizure activity in the right ventral hippocampus. **C** Nissl-stained section reveals long (arrow) and short parts of a bipolar electrode track (double arrow). The short electrode recorded the earliest seizure activity 118 times, which was 96% of all seizures recorded earliest in the right ventral hippocampus and 63% of all seizures recorded in this rat. m = molecular layer, g = granule cell layer, h = hilus, S = subiculum.



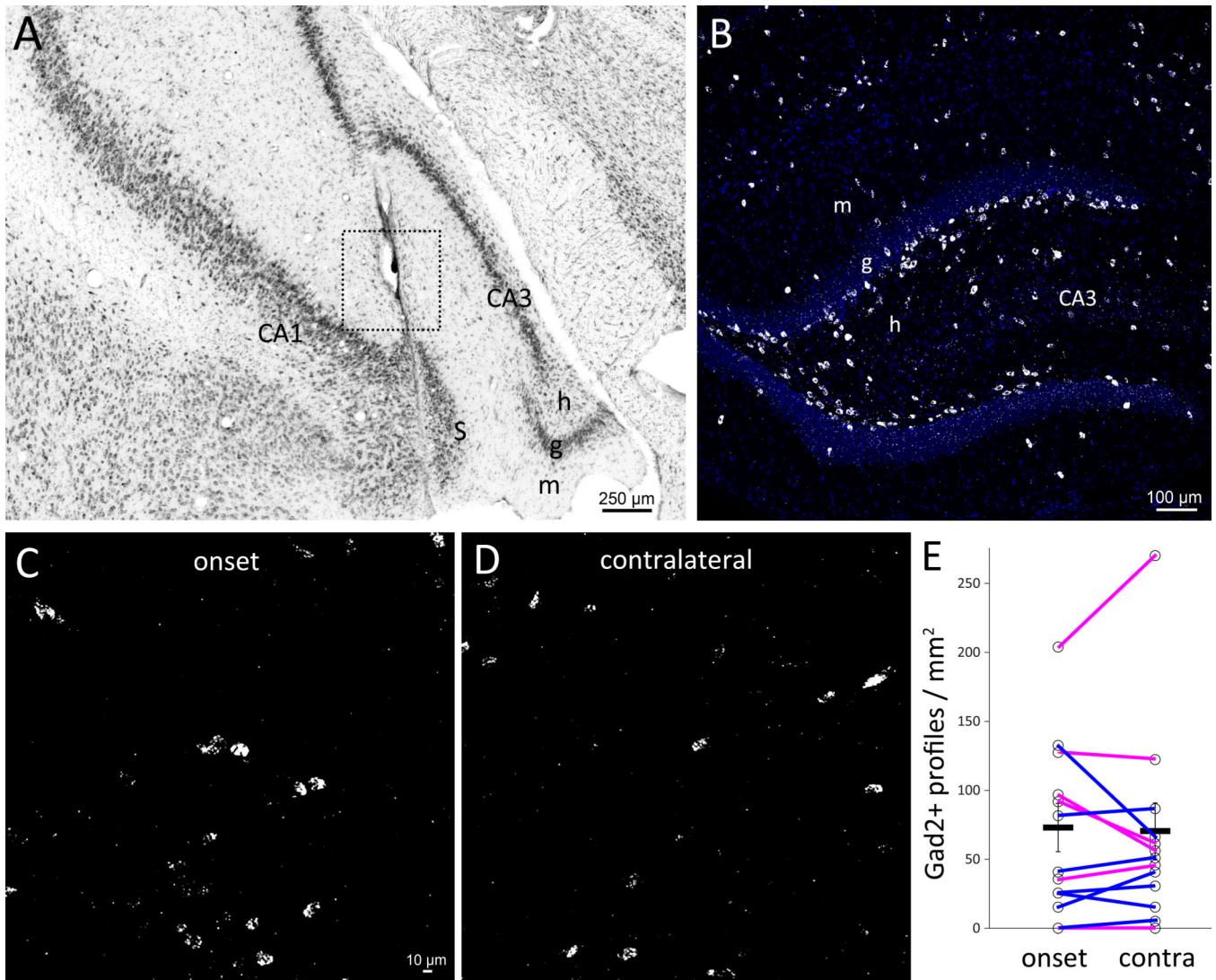


**Figure 3.**

Glutamic acid decarboxylase 2 (*Gad2*) neurons at ictal onset sites. **A** Nissl-stained section with a box denoting a 250 µm radius centered on the electrode tip with the highest z-score for recording earliest seizure activity. m = molecular layer, g = granule cell layer, h = hilus, S = subiculum. **B** *Gad2* neurons in the dentate gyrus of a control rat. DAPI in blue. **C** *Gad2* neurons at the ictal onset site centered on the electrode tip as demarcated in **A** but in a nearby section. **D** *Gad2* *in situ* at the contralateral site. **E** Quantification of *Gad2* neuron profiles at the ictal onset site and contralaterally for each rat. Averages indicated by horizontal black lines. Error bars are s.e.m. Magenta lines indicate rats in which the contralateral site was not a site of significantly earliest seizure activity.

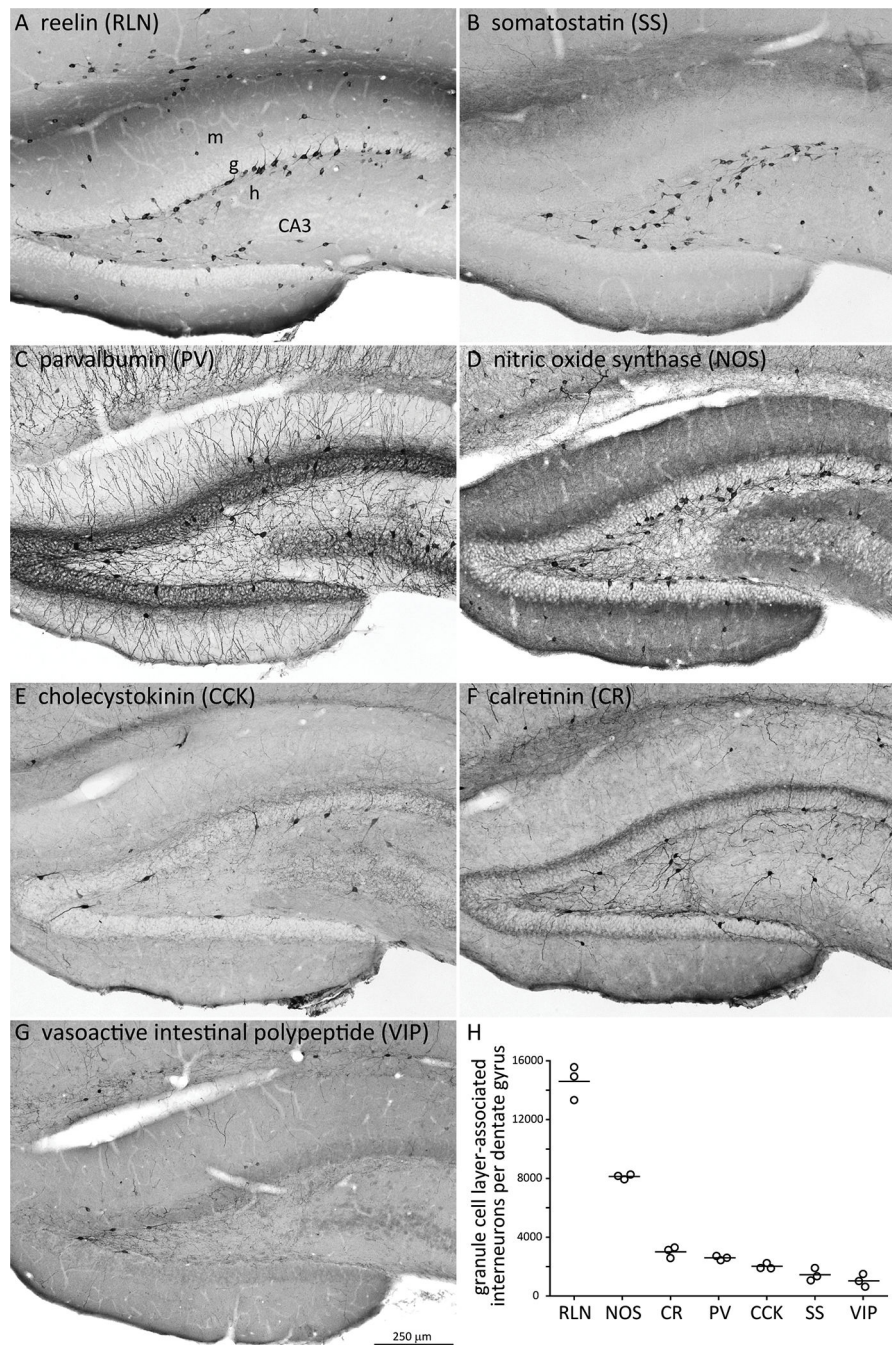


**Figure 4.** Cells that express reelin or nitric oxide synthase account for most granule cell layer-associated interneurons. **A-G** Adjacent hippocampal sections from a control rat processed for different interneuron markers. m = molecular layer, g = granule cell layer, h = hilus. **H** Number of interneurons in or adjacent to the granule cell layer per hippocampus. Circles represent individuals, lines indicate averages.



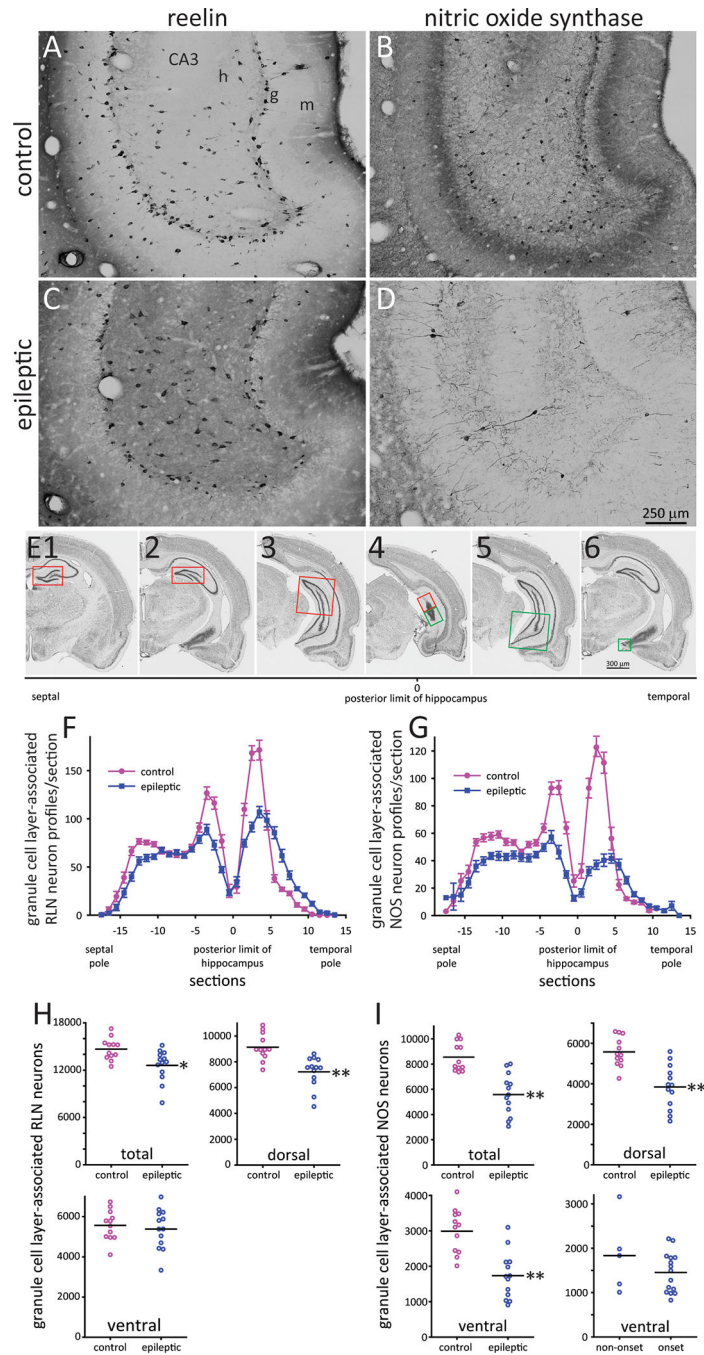


**Figure 5.** Granule layer-associated reelin (RLN)- and nitric oxide synthase (NOS)-immunoreactive interneurons. Ventral hippocampus in a control (A,B) and epileptic rat (C,D). m = molecular layer, g = granule cell layer, h = hilus. E Method to analyze coronal sections. Nissl stained sections from a control rat show the granule cell layer analyzed at different levels of the septotemporal axis of the hippocampus: red outline = septal (dorsal) dentate gyrus; green outline = temporal (ventral) dentate gyrus. E2,6 are the same section. E3,5 are the same section. E4 was the most posterior section that included granule cell layer. Results from the

dorsal and ventral parts of the granule cell layer were plotted as section -1 and 1, respectively, in panels **F,G**. Granule cell layer-associated RLN- (**F**) and NOS-positive neuron profiles/section (**G**). Number of granule cell layer associated RLN- (**H**) and NOS-positive neurons (**I**) in the entire hippocampus (total), dorsal hippocampus, and ventral hippocampus. \* $p < 0.01$ , \*\* $p < 0.001$ , t test. For NOS, there also is a plot of the number in ventral hippocampi of epileptic rats without versus with a significant ictal onset site.

**Table 1**

Number of seizures and electrodes and earliest recorded seizure activity in epileptic pilocarpine-treated rats

rat	# seizures recorded		septum	olfactory cortex	amygdala	dorsal hippocampus	ventral hippocampus	ventral subiculum	entorhinal cortex
1	109	left	2	3	2	2	-	1	2
		right	1	1	3	2	1	2	1
2	186	left	-	1	1	1	1	3	2
		right	2	1	1	3	4	1	1
3	128	left	2	3	-	1	3	-	-
		right	2	3	1	4	4	-	-
4	184	left	-	2	3	2	-	-	3
		right	3	2	2	1	1	1	2
5	109	left	2	2	1	2	3	2	-
		right	2	1	1	1	4	1	1
6	169	left	-	2	2	-	2	1	1
		right	-	-	1	2	1	1	1
7	129	left	-	2	-	2	-	2	1
		right	-	-	1	2	-	1	2
8	186	left	-	1	4	2	2	1	1
		right	2	3	3	3	2	-	-
9	169	left	1	-	1	2	3	3	-
		right	1	1	3	1	-	2	-
10	20	left	-	2	3	2	1	3	-
		right	1	2	2	2	-	2	-
11	24	left	2	2	1	2	2	4	-
		right	1	1	2	2	2	1	2
12	25	left	3	1	1	-	2	1	1
		right	-	1	2	-	2	2	1
13	13	left	3	1	1	2	2	1	1
		right	-	-	1	2	4	-	2

Values indicate number of recording electrodes. Hyphens indicate targeted regions that were not recorded. Brain regions with at least one earliest recorded seizure are highlighted in yellow. Those with significantly more earliest recorded seizures than chance are orange or red (highest z-score for that individual).